

# Electroconsolidation Method for Fabrication of Fine-Dispersed High-Density Ceramics

E.S. Hevorkian<sup>1</sup>, V.P. Nerubatskyi<sup>2</sup>, M. Rucki<sup>3</sup>, A. Kilikevicius<sup>3</sup>, A.G. Mamalis<sup>4</sup>, W. Samociuk<sup>1</sup>, D. Morozow<sup>5</sup>

<sup>1</sup>*University of Life Sciences in Lublin, Lublin, Poland*

<sup>2</sup>*Ukrainian State University of Railway Transport, Kharkiv, Ukraine*

<sup>3</sup>*Vilnius Gediminas Technical University, Vilnius, Lithuania*

<sup>4</sup>*Project Center for Nanotechnology and Advanced Engineering, Athens, Greece*

<sup>5</sup>*Kazimierz Pulaski University of Technology and Humanities in Radom, Radom, Poland*

The paper presents concept and working principle of the electroconsolidation device, which belong to a group of Spark Plasma Sintering (SPS) or Field Activated Sintering Techniques (FAST). Its distinguishing characteristics is the application of the alternating current of high intensity directly to the mould without any sort of pulse generator. Heating process is performed in vacuum, but under uniaxial mechanical pressure applied to the specimen. Some issues concerning the current passing through the powders and subsequent densification with related porosity, strength and hardness of the sintered structures were discussed. It was found that apart from the simplified construction, the high heating rates, short holding time and relatively low sintering temperatures were resource saving and contributed to the greener manufacturing of advanced nanostructural composites.

**Keywords:** Powder metallurgy; electroconsolidation; sintering; ceramics.

## 1. Introduction

While there is an increasing need of nanostructural composites in large variety of technical and bioengineering applications [1], the directions of development known as Industry 5.0 concepts have clear and direct references to the environmental issues and limitations of the resources of our planet, which is emphasized by the European Commission and other institutions [2].

Among fabrication methods of nanocomposite materials, the powder metallurgy is one of the most important, since it makes possible to control the structural features during manufacturing process [3]. This paper is dedicated to the electroconsolidation method, which

is feasible for fabrication of nanostructural materials and composites [4, 5]. In the method, the hot pressing is utilized, but the sole heat source for sintering process is the electrical current, directly applied to the sintered object. It will be demonstrated that the method is worthy to be developed and investigated since it is advantageous compared to other powder metallurgy techniques. It is simple and efficient, does not require complicated and advanced apparatus, provide high heating rates and short holding times. As a result, fine-dispersed structural features can be obtained that exhibit equal and sometimes better characteristics than the structures obtained from similar materials by other powder metallurgy methods.

Further improvement of physical and mechanical characteristics is possible, but it require research and understanding of the following:

- role of the electrical discharge in the porosity removal during the electroconsolidation process, in particular, how the process is dependent on the current parameters, its supply to the graphite mould, and the sintering environment;
- dependence between resulting structural features and heating rates, holding time and temperature, etc.;
- possibility to sinter powders of different electrical activities and specific surface areas.

Noteworthy, the submicron powders require much lower temperatures than that of traditional powders sintering. Among the problems to be solved is agglomeration of the powders before sintering. Thus, it is necessary to find the method of refinement in order to obtain repeatable, homogenous structures. Moreover, for the successful, wide application of the method, it is necessary to pay attention to the following:

- modelling the process of pore formation;
- understanding of the formed pore species, in terms of expected porosity, pore shapes and dimensions;
- modelling and simulation of the temperature distribution inside the graphite moulds;
- analysis of structural formation at different process parameters;
- optimization of the sintering parameters for different types of the powder mixtures.
- obviously, electrical discharges between the surfaces of the particles depend on the properties of the components, powder morphology and size, gaseous environment, mechanical pressure and current parameters. Understanding of the complex phenomena is possible due to combination of knowledge in the areas of applied physics, mathematics, chemistry, and materials sciences.

## **2. Materials and methods**

In the literature, hot pressing, hot isostatic pressing, and spark plasma sintering (SPS), including hybrid SPS + resistance/induction heating methods, are often named among the techniques applied for the development of nanocrystalline materials [6]. In fact, there are many sintering techniques activated by the electric current (ECAS), where an electric current

*Nanotechnology Perceptions* Vol. 20 No.1 (2024)

is used to generate heating in a conductive mould, while a uniaxial mechanical load is being simultaneously applied to the specimen [7]. Among the ECAS methods, the following can be named, as reported shortly after invention:

- Field Activated Sintering Technique, FAST (USA) [8];
- Spark Plasma Sintering, SPS (USA, Japan) [9];
- High Pressure Spark Plasma Sintering, HPSPS (USA) [10];
- Plasma Activated Sintering, PAS (Japan, USA) [11];
- Pulse Electric Current Sintering, PECS (Japan) [12];
- Plasma Pressure Compaction, PPC (USA) [13];
- Instrumented Pulse Electro-Discharge Consolidation, PEDC (Japan) [14];
- Resistance Pressing Sintering, RPS (China) [15];
- Field-Activated Pressure-Assisted Synthesis, FAPAS) (France, USA) [16, 17].

Since there are only slight differences between the techniques, many authors do not distinguish between them, referring to as SPS or FAST [18-20]. In this context, the electroconsolidation technique is distinct due to the alternating current applied directly to the graphite mould, without any sort of pulse generator [21]. Simplification of the construction, as well as of the process itself, meet the requirements of both Industry 4.0 concerning the efficiency and of the Industry 5.0 concerning sustainability and resource saving [22, 23]. In this paper, we will discuss some peculiarities of the electroconsolidation process and its influence on the final properties of the sintered materials.

### **3. Theoretical background**

To realize the concept of electroconsolidation, the following prototype apparatus was built up, as shown in Figure 1. It consisted of the main body (1), upper and lower power conductors (2 and 3, respectively), sealing (4), thermocouple (5), pressing bodies (6), mould matrix (7), mould shell (8), and radiation shield (10). The powder is placed in the area (9), where it undergoes mechanical pressure and high current through the conducting elements (6, 7, 8). Before starting the process, the air is removed from the camera (1), leaving the vacuum of  $10^{-3}$  Pa.

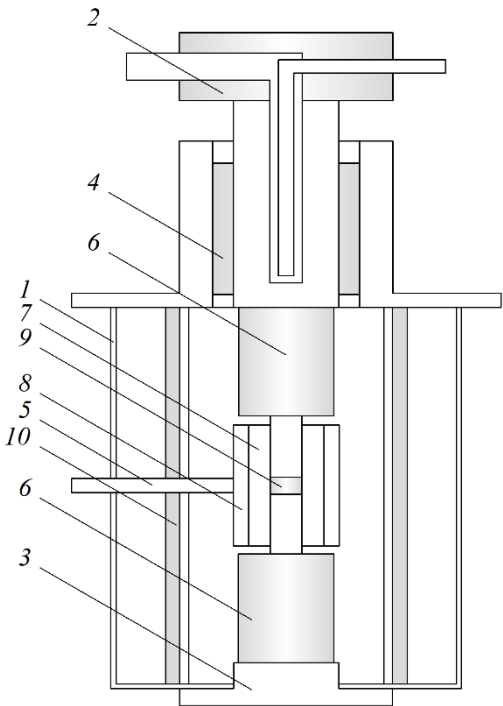


Figure 1. Scheme of the prototype device

In the electroconsolidation process, the alternating electric current is the sole heat source. It was found sufficient to use a typical mains transformer, which reduced the voltage down to ca. 10 V with high current of up to 9 kA.

Since the high current caused heating of the contact surfaces, it was necessary to apply a water cooling system of all the flexible conductors, as well as the outer surface of the main body. The current flow through the mould and the powder sample is controlled by a unit that regulates the current in the primary winding of the transformer. This way it is possible to control the temperature and heating rate with high accuracy, and to make necessary adjustments during the sintering process. To collect the information on the compaction process, the system of sensors was built, as shown in Figure 2. It allowed for measurement of the mechanical pressure  $P$ , relative compaction  $\Delta L/L_0$ , and temperature  $T$ , to process it with AVR microcontroller (MC), and then to record and analyze the data using a PC.

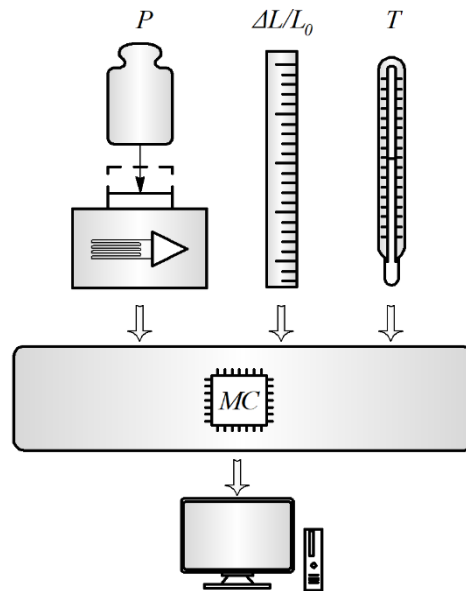


Figure 2. Block-scheme of the measurement and control system

To control the mechanical pressure  $P$ , a dedicated deformation measurement system based on strain gauges was built. Its main component was a hollow steel cylinder (1) closed in the housing (4), as shown in Figure 3, A.

On the surface of the cylinder, strain gauges were placed in the coaxial direction  $R_{\parallel}$  (2) and perpendicularly to the cylinder's axis  $R_{\perp}$  (3). Their connection in a Wien bridge electrical circuit is shown in Figure 3, B.

Under the mechanical pressure applied to the mould, the deformed cylinder caused changes in the coaxial strain gauge resistance  $R_{\parallel}$  (2). The signal was amplified using very sensitive device AD8221, which registered even very small drifts of zero. In order to minimize the error, the reference strain gauges were placed near by, but on the surface not deformed. The amplifier was assembled on a small printed circuit board of dimensions 31×23 mm placed inside the housing.

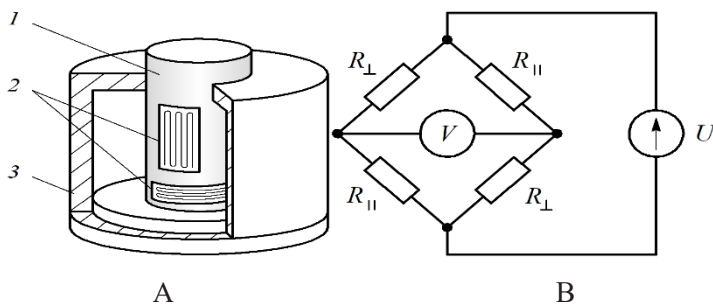


Figure 3. Measurement of the pressing force:

(A) position of the strain gauges, (B) connections in the circuit

The compaction of the sample was measured in terms of linear shrinkage related to the initial length  $\Delta L/L_0$ . The linear optical encoder was fixed on the frame, while the optical sensing head was fixed to the upper conducting element (2) shown in Figure 1. This solution provided measurement of the linear displacement with accuracy of 70  $\mu\text{m}$  in the wide range of positions. There was no need of calibration, and the output digital signal did not require amplification.

Since the temperature could not be measured directly inside the mould, a tungsten-rhenium thermocouple BP-5/20 was placed in its peripheral area. An optical pyrometer was used for the calibration, and the temperature was measured in the range between 20 °C and 2000 °C with accuracy of 1 °C. From the measurement results, the temperature inside the mould was calculated using finite elements method (FEM), modelling the distribution of the temperature in the critical points.

The microcontroller was able to register four parameters simultaneously: mechanical pressure  $P$ , linear displacement  $\Delta L$ , temperature  $T$ , and the time  $t$ . With the given sampling interval, these data were collected and forwarded to the main PC in a real-time mode, creating a file for further analysis. The actual values of pressure and temperature are also shown in the display. The MC was programmed with a firmware using C programming language, where USB 2.0 interface is implemented in software. This interface made it possible to connect any PC to the system.

#### **4. Results and discussion**

The experiments with electroconsolidation in vacuum for the powder non-conductive materials demonstrated that the obtained microstructure was very sensitive to the sintering temperature and the holding time. The thermal fields during heating exhibited gradients and heterogeneity of the temperature distribution, which can be attributed to the effect of the electric discharge processes in a graphite mould. Figure 4 presents dynamical changes of the temperature gradients in the pressed volume during sintering.

Due to many factors, the difference between the model and real temperature changes is quite large in the heating and cooling time span. One of the main factors is higher thermal inertia of the real system, which can be corrected in the model in future research. After 400 s, when 90 % of the maximal temperature was reached, the heating rate was slowed down, and the difference between the model and the measurement dropped below 10 %. The sintering period between 600 s and 1000 s exhibited very high conformity of the model, and the temperature was kept almost unchanged at the level of 1200 °C.

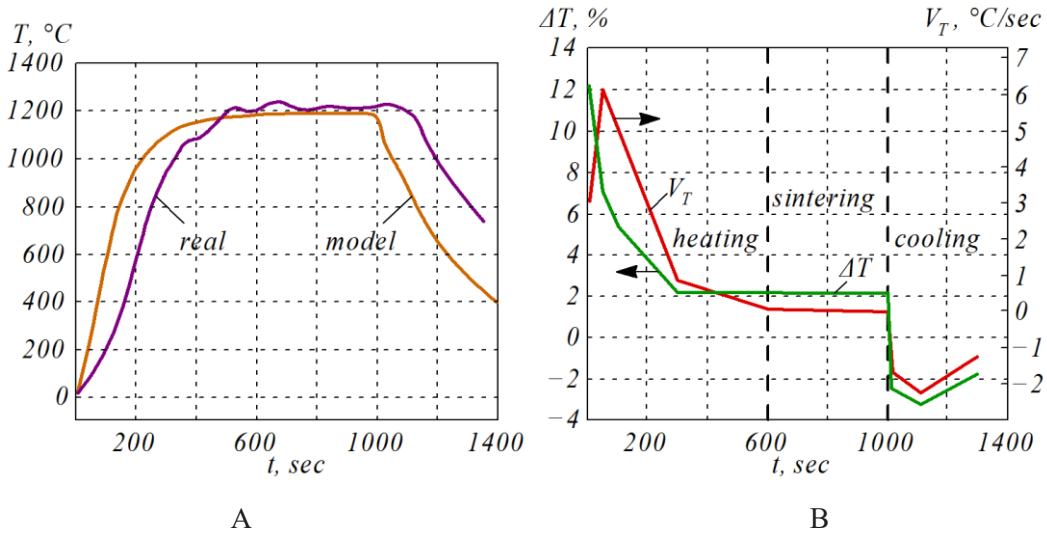


Figure 4. Temperature during the sintering process:

(A) comparison between the model and measurement of temperature, (B) correlation between the heating rate  $V_T$  and temperature increment  $\Delta T$

Based on the specific features of the electroconsolidation method, all the heat should be transferred to the sintered sample and form along it a temperature gradient. However, the heat may also dissipate to the environment, which is limited by vacuum chamber. Moreover, heat transfer by radiation grows more significant with increase of the temperature, since its magnitude is dependent on the thermal stage of the radiating body (defined by temperature, emissivity, radiosity, reflexivity), on its geometrical features (shape and segmentivity), and on the quality of the emitting surface (smoothness, roughness, colour). In the proposed device, radiation is the dominant way of the heat transfer, with radiation wavelengths within the range of 1.6...3.2  $\mu\text{m}$  at temperatures between 600 °C and 1500 °C [24]. This problem was solved using the radiation shield marked (10) in Figure 1, which “doubled” the infrared radiation inside the chamber, minimizing the respective heat losses.

During the neck formation between the particles sintered under electric current, the following phenomena take place [25]:

- vaporisation and solidification;
- volume diffusion;
- surface diffusion;
- grain boundary diffusion.

Presumably, electric current flow through a powder caused enhanced lattice vibration energy in the defect vicinity [26]. The local Joule heating in SPS methods provides a greater amount of energy directly to the dislocations. As a result, dislocations can move more easily and the stress required is reduced with heating at the atomic level contributing to the total heating of

the sample. Hence, both local Joule heating effect and electron wind effect possibly contributed to the sintering under electric current.

The analysis of sintering process in SPS revealed that grain boundary diffusion was the main densification mechanism. Moreover, electrical discharge presumably may contribute to the cleaning of the particle surface [27] and creation of the surface defects. These defects may work promoting the grain boundary diffusion due to the additional free volume  $\Delta\alpha$  [28].

Considering the powder mixture like ceramic-metal composite, where one component is a conductor while the other is a non-conductive material, Figure 5 shows a schematic current route. Apart from the particles, the pores are involved in the process, and should be taken into account as capacitors in the electrical equivalent.

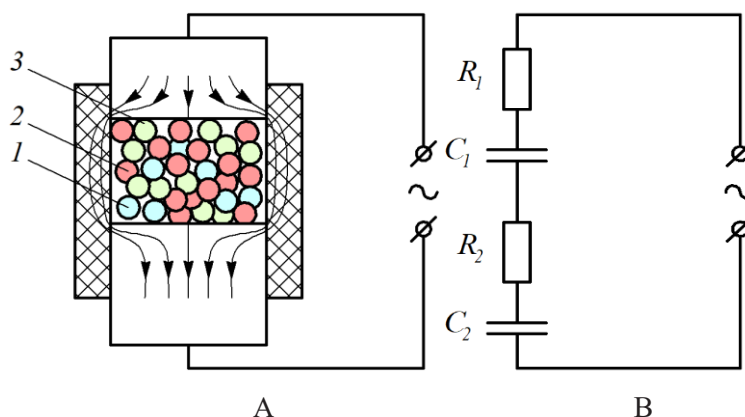


Figure 5. The electric current passing through the mixture of conductive powder (1) of resistance  $R_1$ , non-conductive powder (2) of resistance  $R_2$ , and pores (3) of capacitance  $C_1$  and  $C_2$ :

(A) conceptual scheme, (B) electric connections

At room temperature, gases are excellent insulators, but a sufficient number of charge carriers can make the gas to conduct electrical current. This process is referred to as electrical breakdown leading to the creation of a conducting path. When the electrical current is passing through the gap between the electrodes, the gaseous discharge phenomena takes place [29, 30]. Three types of discharges can be distinguished, dependent on the current: dark or Townsend discharge, glow discharge, and arc discharge, as shown in Figure 6.

At some point corresponding with a critical breakdown voltage, there is a sudden transition from a small, dark current to the self-sustaining discharge. Transition from the dark discharge to the glow one is accompanied by the dramatic increase of the current. Usually, the discharge phenomena take place at constant voltage, but the gas discharges take place also at alternating one, and they remain stationary, when the frequency is high enough. This is known as an electrodeless discharge phenomenon in a gas at low pressure, generated by a high-frequency electric field [31].

In the electroconsolidation device, an alternating electric field creates plasma in a certain



volume and transfers sufficient energy to electrons to maintain ionization, compensating for the loss of charged particles due to diffusion and recombination.

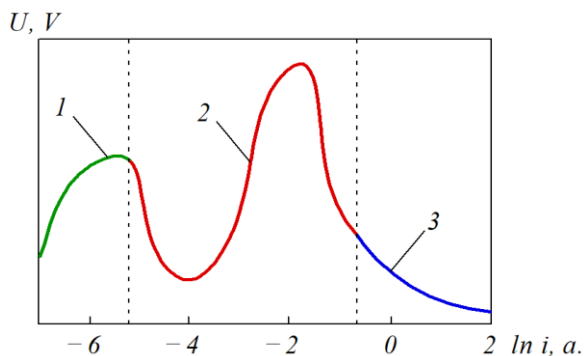


Figure 6. A current–voltage characteristic of a gas:

1 – dark discharge, 2 – glow discharge, 3 – arc discharge

The appearance and characteristics of high-frequency discharges depend on the type of gas, its pressure, the frequency of the alternating electric field and the transmitted power. Among effects of the electric field on the sintering process, the local field intensification should be named, but also electromigration and electrowetting.

These phenomena contribute to the complex process of SPS and electroconsolidation, and their effect is dependent on the current and voltage, powder composition, gaseous environment and pressure, etc. In different conditions, different factors may become dominant, forming diffusional and viscous flows in grain boundary sliding process, dislocations, deformations and diffusion [32]. As a result, different kinetics of the densification and grain growth with respective alteration of the sintered structural features would provide different physical and mechanical characteristics of the obtained material.

It should be mentioned also that the heating rate, which is directly dependent on the applied current, had substantial effect on the densification process. Not only holding temperature was  $T_{\text{ sint}}$ , but also different heating rates contributed to the relative density  $\rho$  of the compacted materials, as it is illustrated in Figure 7.

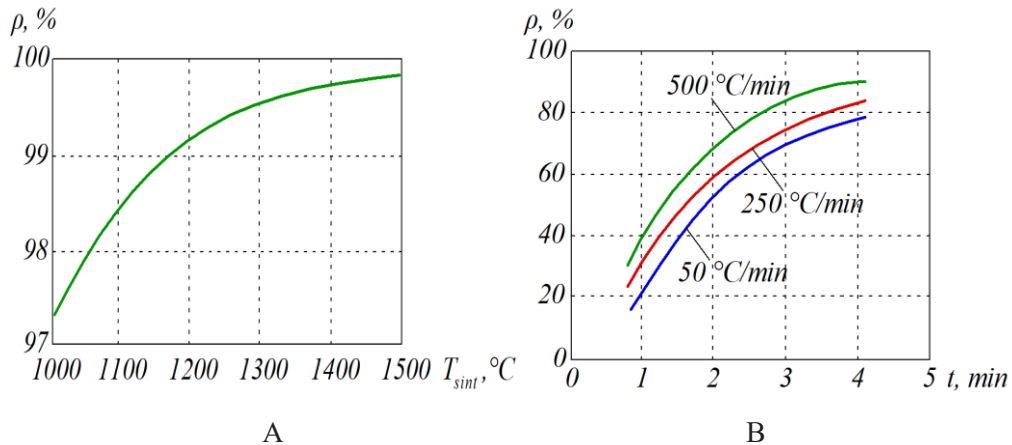


Figure 7. The effects on the powder densification:

(A) mixture of  $Al_2O_3$  with 50wt.% WC, sintered at  $P = 45$  MPa and different  $T_{sint}$ ,

(B) mixture of  $Al_2O_3$  with 10wt.% SiC, sintered at  $T_{sint} = 1500$  °C,  $P = 45$  MPa, and different heating rates

Figure 7, A shows the effect of on the sintered mixture of  $Al_2O_3 + 50$ wt.% WC, while Figure 7, B presents the effect of heating rate on the mixture of  $Al_2O_3 + 10$ wt.% SiC, sintered at holding temperature  $T_{sint} = 1500$  °C, and pressure  $P = 45$  MPa.

In general, the quicker heating, the better was compaction, and the higher holding temperature, the closer relative density to 100 %. However, it appeared that the full densification is not always advantageous. For instance, tungsten carbide WC sintered at temperature  $T_{sint} = 1800$  °C exhibited higher porosity than that sintered at  $T_{sint} = 1730$  °C, as shown in Figure 8, A, but due to the grain growth, its flexural strength dropped down, as seen in Figure 8, B.

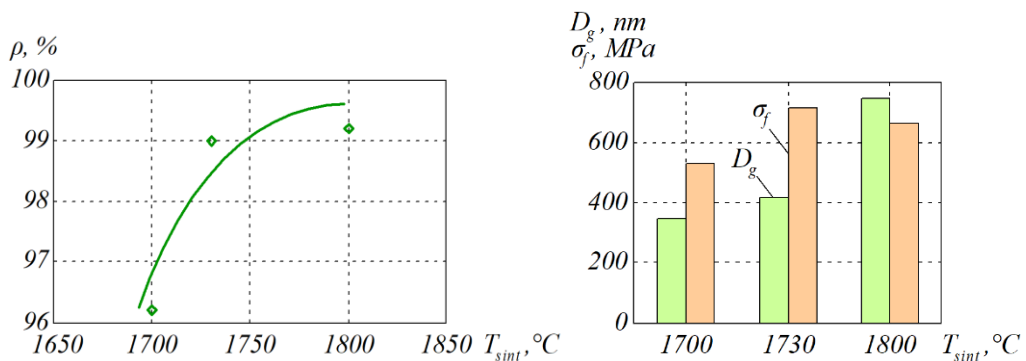


Figure 8. The effect of the sintering temperature on the WC powder densification:

(A) relative density % $\rho$  achieved at different  $T_{sint}$ , (B) average grain size  $D_g$  and flexural strength  $\sigma_f$  achieved at different  $T_{sint}$

The holding time is also an important factor contributing to the grain growth in the sintered material, weakening its mechanical characteristics. In the case of 3 mol% yttria stabilized  $\text{ZrO}_2$  mixed with 50 wt.% WC, grain size  $D_g$  grew very fast when holding time was prolonged above 5 minutes at  $T_{\text{sint}} = 1700^\circ\text{C}$  and  $P = 40\text{ MPa}$  (Figure 9, A).

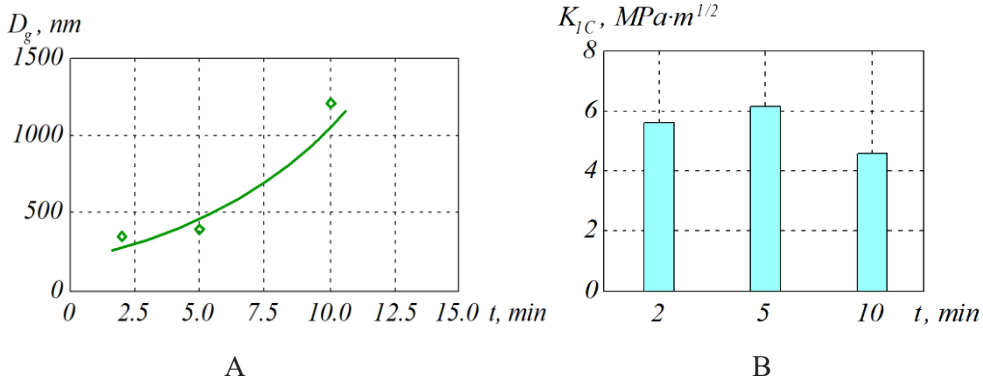


Figure 9. The effect of the holding time on the 3 mol%  $\text{Y}_2\text{O}_3$  stabilized  $\text{ZrO}_2 + 50\text{ wt.}\%$  WC powder densification: (A) grain size  $D_g$ , (B) fracture toughness  $K_{IC}$

At the same time, fracture toughness  $K_{IC}$  dropped substantially, as it is seen in Figure 9, B. These parameters of electroconsolidation process are of particular importance in the case of certain materials.

For instance, when preparing the composites with diamond reinforcement, short holding time and relatively low temperatures prevent from graphitization but ensure full density [33]. In terms of technical data, available heating rates and pressure, it can be seen from Table 1.

Table 1. Comparison of different methods

Method	Pressure, GPa	Temperature, $^\circ\text{C}$	Relative density, %	Heating rate, $^\circ\text{C/s}$	Holding time, s
Hot Isostatic Forging (HIF)	1.0	1200...1500	$\geq 95$	10...20	120...300
Quick Hot Isostatic Pressing (QHIP)	1.0	1500...2000	$\leq 95$	20...30	60...300
FAST/SPS	0.06	$\leq 2200$	$\geq 95$	20...30	180...300
High Energy High Rate compaction (HEHR)	1.5	$\leq 3400$	$\leq 98$	20...30	100...120
Upgraded Field Assisted Sintering Technology (U-FAST)	26.0	$\leq 2000$	94...98	3...4	300...600
Electroconsolidation under AC	0.45	2200	99	5...10	120...180

Electroconsolidation is comparable or sometimes better than that of other commonly known sintering methods.

## 5. Conclusions

The presented electroconsolidation method appears to be advantageous in terms of simple construction and operation. On the other hand, the obtained submicron structures are advantageous or comparable to those obtained by other techniques. Future research will focus on the specific compositions as well as on the theoretical explanation and modelling of the physical phenomena accompanying the process.

Acknowledgements: This work has been funded from the MSCA4Ukraine project, which is funded by the European Union.

Note, however, that the two already published Papers:

1. A.G. Mamalis, E.S. Hevorkian, V.P. Nerubatskyi, M. Rucki, Z. Krzysiak and O.M. Morozova, "Effect of nano additives on the properties of partially stabilized zirconia", *Nanotechnology Perceptions*, Vol. 19, No. 3, pp. 26/46, 2023
2. A.G. Mamalis, E.S. Hevorkian, V.P. Nerubatskyi, Z. Krzysiak, O.M. Morozova and L.Chalko, "Peculiarities of obtaining nanostructured materials compacted by the method of hot pressing due to the passage of direct electric current" *Nanotechnology Perceptions*, Vol. 20, No. 1, pp. 61/71, 2024

have been also co-funded from the same MSCA4Ukraine Project, which is funded by the European Union, and the Ministry of Education and Science of Ukraine Project No. 0121U109441.

## References

1. Gniadek, M., et al., *Influence of nanostructural additives on the properties of polypyrrole-based composites*. *Journal of Electroanalytical Chemistry*, 2023. **938**: p. 117409.
2. Mesjasz-Lech, A., *Can Industry 5.0 be seen as a remedy for the problem of waste in industrial companies?* *Procedia Computer Science*, 2023. **225**: p. 1816-1825.
3. Zhang, Y., et al., *Mechanical behavior of Pt-graphene porous biocompatible nanocomposites prepared by powder metallurgy using molecular dynamics simulation*. *Journal of Molecular Liquids*, 2022. **360**: p. 119450.
4. Krzysiak, Z., et al., *Peculiarities of the phase formation during electroconsolidation of Al<sub>2</sub>O<sub>3</sub>-SiO<sub>2</sub>-ZrO<sub>2</sub> powders mixtures*. *Materials*, 2022. **15**(17): p. 6073.
5. Nerubatskyi, V., et al., *Investigation of the effect of silicon carbide nanoadditives on the structure and properties of microfine corundum during electroconsolidation*. *Low Temperature Physics*, 2023. **49**(4): p. 498-498.
6. Babalola, B.J., O.O. Ayodele, and P.A. Olubambi, *Sintering of nanocrystalline materials: Sintering parameters*. *Heliyon*, 2023. **9**(3).
7. Ratzker, B. and M. Sokol, *Exploring the capabilities of high-pressure spark plasma sintering (HPSPS): A review of materials processing and properties*. *Materials & Design*, 2023: p. 112238.
8. Anderson, K., et al., *Surface oxide debonding in field assisted powder sintering*. *Materials Science and Engineering: A*, 1999. **270**(2): p. 278-282.

9. Omori, M., A. Okubo, and T. Hirai, *Si<sub>3</sub>N<sub>4</sub>-Y<sub>4</sub>Al<sub>2</sub>O<sub>9</sub> Composites Prepared by Spark Plasma Sintering*, in *Advanced Materials' 93*. 1994, Elsevier. p. 887-890.
10. Anselmi-Tamburini, U., J. Garay, and Z.A. Munir, *Fast low-temperature consolidation of bulk nanometric ceramic materials*. Scripta materialia, 2006. **54**(5): p. 823-828.
11. Tracy, M. and J. Groza, *Nanophase structure in Nb rich-Nb<sub>3</sub>Al alloy by mechanical alloying*. Nanostructured Materials, 1992. **1**(5): p. 369-378.
12. Yoshimura, M., et al., *Synthesis of nanograined ZrO<sub>2</sub>-based composites by chemical processing and pulse electric current sintering*. Materials letters, 1999. **38**(1): p. 18-21.
13. Yoo, S.H., et al., *Consolidation and high strain rate mechanical behavior of nanocrystalline tantalum powder*. Nanostructured Materials, 1999. **12**(1-4): p. 23-28.
14. Kimura, H., *Synthesis of nano-structured high-temperature titanium aluminide by instrumented pulse electro-discharge consolidation of mechanically alloyed amorphous powder*. Le Journal de Physique IV, 1993. **3**(C7): p. C7-423-C7-428.
15. Hu, J., et al., *The initial powder-refinement-induced donor-like effect and nonlinear change of thermoelectric performance for Bi<sub>2</sub>Te<sub>3</sub>-based polycrystalline bulks*. Semiconductor Science and Technology, 2017. **32**(7): p. 075004.
16. Bernard, F., et al., *Dense nanostructured materials obtained by spark plasma sintering and field activated pressure assisted synthesis starting from mechanically activated powder mixtures*. Science of Sintering, 2004. **36**(3): p. 155-164.
17. Gauthier, V., et al., *Synthesis of nanocrystalline NbAl<sub>3</sub> by mechanical and field activation*. Intermetallics, 2001. **9**(7): p. 571-580.
18. Cepeda-Jiménez, C.M. and M.T. Pérez-Prado, *4.12 Processing of Nanoparticulate Metal Matrix Composites*. 2018.
19. Laszkiewicz-Łukasik, J., et al., *Spark plasma sintering/field assisted sintering technique as a universal method for the synthesis, densification and bonding processes for metal, ceramic and composite materials*. Journal of Applied Materials Engineering, 2020. **60**.
20. Hu, Z.-Y., et al., *A review of multi-physical fields induced phenomena and effects in spark plasma sintering: Fundamentals and applications*. Materials & Design, 2020. **191**: p. 108662.
21. Gevorkyan, E., et al., *Structure formation in silicon carbide–alumina composites during electroconsolidation*. Journal of Superhard Materials, 2022. **44**(5): p. 339-349.
22. Golovianko, M., et al., *Industry 4.0 vs. Industry 5.0: co-existence, Transition, or a Hybrid*. Procedia Computer Science, 2023. **217**: p. 102-113.
23. Gevorkyan, E., et al., *Smart Sustainable Production Management for City Multifloor Manufacturing Clusters: An Energy-Efficient Approach to the Choice of Ceramic Filter Sintering Technology*. Energies, 2022. **15**(17): p. 6443.
24. Zhou, X., et al., *Enhanced radiation heat transfer performance of Alumina-Spinel composite sphere with hollow structure for rapidly ultra-high temperature thermal storage/release process*. Chemical Engineering Journal, 2024. **479**: p. 147381.
25. Nee, A.Y.C., *Handbook of manufacturing engineering and technology*. 2014: Springer Publishing Company, Incorporated.

26. Lee, G., et al., *Effect of electric current on densification behavior of conductive ceramic powders consolidated by spark plasma sintering*. Acta Materialia, 2018. **144**: p. 524-533.
27. Wu, M., et al., *Direct evidence for surface cleaning mechanism during field-activated sintering*. Journal of Alloys and Compounds, 2019. **784**: p. 975-979.
28. Mehrer, H., *Diffusion in solids: fundamentals, methods, materials, diffusion-controlled processes*. Vol. 155. 2007: Springer Science & Business Media.
29. Mamalis, A., et al., *Peculiarities of the formation of the structure of CMCs based on Al<sub>2</sub>O<sub>3</sub> micropowder and SiC nanopowder in the process of electrosintering*. Nanotechnology Perceptions, 2023. **19**(2): p. 39–53-39–53.
30. Boulos, M.I., P.L. Fauchais, and E. Pfender, *Basic concepts of plasma generation*, in *Handbook of Thermal Plasmas*. 2023, Springer. p. 473-506.
31. Francis, G., A. Von Engel, and F.A. Lindemann, *The growth of the high-frequency electrodeless discharge*. Philosophical Transactions of the Royal Society of London. Series A, Mathematical and Physical Sciences, 1953. **246**(909): p. 143-180.
32. Gevorkyan, E., et al., *Analysis of the electroconsolidation process of fine-dispersed structures out of hot pressed Al<sub>2</sub>O<sub>3</sub>–WC nanopowders*. Materials, 2021. **14**(21): p. 6503.
33. Ratov, B., et al., *Features Structure of the Cdiamond–(WC–Co)–ZrO<sub>2</sub> Composite Fracture Surface as a Result of Impact Loading*. Journal of Superhard Materials, 2023. **45**(5): p. 348-359.